On the Arrangements of the Micro-Crystals in Bismuth and Antimony deposited by Electrolysis[1]

By

Hideki Hirata

(Received July 9, 1928)

Abstract

The arrangements of the micro-crystals in electrolysed specimens of bismuth and antimony, deposited under various conditions, were examined with X-rays, by the so-called "transmission method." The diffraction-patterns thus obtained were seen to be explainable by the following considerations:- (1) The formation of the regular arrangements of bismuth crystals seems to be influenced at least by two factors: i.e., the current density and the concentration of the electrolyte. The smaller current density and the lower concentration of the electrolyte seem to be the favorable conditions for the formation of regular arrangement. (2) The non-metallic cloddy deposits found on the cathode by the electrolysis of bismuth or antimony, are composed mainly, at least, of the micro-crystals having the same space lattices respectively as those of bismuth or antimony. (3) The micro-crystals of bismuth in its fibrous specimen are so arranged that the crystal-axis[2] of the indices [211] is parallel to the axis of the fibre. Not only in the fibrous specimens, but also in the single crystals of bismuth obtained in an acicular form, the same crystal-axis is parallel to the direction of the acicular axis.

Introduction

Up to now, a number of investigations have been carried out in connection with the crystalline structures of electrodeposited metals, by making use of the diffraction phenomena of X-rays. As the results of these researches, it has generally been accepted that the micro-crystals

1 This was read in part at the meeting of the Chemical Society of Japan, April, 1927.

2 Following Niggili, the indices of a direction in the crystal are represented by its direction ratios h k l with respect to the three rhombohedral edges of the crystal of bismuth. This direction is called, in this paper, the crystal-axis bearing the indices [h k l].

of an electrolytically deposited metal have the tendency to arrange themselves in a fibrous form, on the one hand,[1] while, on the other, they precipitate without any regularity under certain circumstances.[2] Quite recently it has however been found that the formation of single crystals by electrolysis is also possible in a certain condition.[3]

Thus, in the present investigation of crystal structures, it seems to be of vital importance to distinguish the conditions, under which the different arrangements of the micro-crystals are produced. It may also be suggestive to compare the orientations of crystal-axes in various electrodeposited metals for the furtherance of investigations.

Only a few experimental data are however available for our consideration. Especially, with regard to electrodeposited metals belonging to some peculiar lattice-forms such as bismuth and antimony, no datum has as yet been obtained up to the present time. So, the writer was induced to start the experiments with electrolytic bismuth and antimony. The procedure of obtaining the specimens is described below.

Experimental Part

Specimen. The specimens used in this experiment were deposited on a thin electrolytic sheet copper 14 cm.^{2} in area as the cathode. A cast plate of bismuth or antimony of the same size served as the anode. Two electrodes were suspended parallel to each other at a distance of about 2·5 cm., and the potential difference applied to them was 2 volts for bismuth and 4 volts for antimony.

The specimens were deposited, usually, in a cloddy form like platinum black, but in a few special cases, where the current density and the concentration of electrolyte were small, the specimens with the proper metallic lustre of bismuth or antimony in very minute acicular or lamellar forms (0·7—1·2 mm. in diameter) came to appear mixed with the cloddy specimens.

Let us designate the metallic specimen as Specimen-A, and the cloddy one as Specimen-B, and for their sub-classes with different numerical suffixes, as A_1, A_2, B_1, B_2, etc.

1 R. Glocker u. K. Kaupp: Z. S. f. Phys., **24**, 121 (1924).
Richard M. Bozorth: Phys. Rev., **26**, 390 (1925).

2 R. Glocker u. K. Kaupp: Loc. cit.
Richard M. Bozorth: Loc. cit.

3 G. Asahara and T Sasahara: Scientific Papers of the Institute of Physical and Chemical Research, **5**, 79 (1926).

The conditions, under which these specimens were obtained, are given below :–

Bismuth.

Specimens A_1 and B_1

Electrolyte : 42 ccs. of HCL, 178 ccs. of H_2O, and 18 grams of No_3 (OH_2) Bi.

Current density : 0·07 amp./cm.^{2}

Specimens A_2 and B_2

Electrolyte : 84 ccs. of HCL, 356 ccs. of H_2O, and 18 grams of NO_3 (OH_2) Bi.

Current density : 0·036 amp./cm.^{2}

In the above two cases, the most part of the deposit was the cloddy Specimen B, the metallic Specimen A being very scarce.

Specimens A_3 and B_3

Electrolyte : 84 ccs. of HCL, 356 ccs. of H_2O, and 9 grams of NO_3 (OH_2) Bi.

Current density : 0·025 amp./cm.^{2}

The specimens obtained were mostly of the metallic Specimen A.

Specimen B_4

Electrolyte : The same as with A_1 and B_1.

Current density ; 0·036 amp./cm.^{2}

In this case, the specimen with the metallic lustre could hardly be detected.

Antimony.

Specimens A_2 and B_2.

Electrolyte : 113 grams of K_2CO_3, 54 grams of Sb_2S_3, and 1 litre of H_2O.

Current density : 0·036 amp./cm.^{2}.

In this case the electrolyte was prepared according to the following procedure :

The mixture described above was boiled about one hour. Its concentration was kept unchanged during the boiling by adding now and then as much water as was lost by evaporation. The filtrate obtained from the boiled solution was left to cool gradually, and then used as its electrolyte.

Specimen B_1: In this case the electrolyte was prepared in the same way as with Specimen A_2 and B_2, and kept boiling during the process of the electrolysis,

What has been described above, can be summarized as follows : with respect to bismuth and antimony, a specimen represented by a

smaller numerical suffix corresponds generally to a larger current density and to a larger concentration of the electrolyte. The only exception to the above is the Specimen B_4 of Bi. In this case, the current density and the concentration of the electrolyte were larger than those corresponding to Specimen-B_3 and Specimen-A_3 of Bi.

The micro-photographs of various specimens are reproduced in Plate I.

Outline of the Experimental Method. In the present experiment the writer adopted the ordinary "transmission method", and it was essentially the same as that previously employed by H. Komatsubara and the present writer[1] to examine electrolysed silver.

The heterogeneous X-rays emitted from the molybdenum-anticathode of Coolidges U-type tube were confined to a narrow circular beam by letting them pass through narrow circular holes in two lead diaphragms. And the specimen to be tested was illuminated by this narrow beam of X-rays. To obtain the diffraction figure, a photographic plate was always placed perpendicularly o the incident beam in a position 3·2 cms. behind the specimen, unless otherwise stated. The maximum voltage applied to the tube was about 50-80 K.Vs., and the current through it was 4-5 milliamperes.

By the electrolysis of bismuth and antimony, it was very difficult to get a good specimen of moderate size and of a suitable thinness for X-ray examination. A slight increase in its thickness would considerably reduce the intensity of the diffracted rays. Thus, most of the specimens gave very diffuse, sometimes too diffuse to be reproduced, diffraction figures.

So, it seems to be of fundamental importance to select specimens profitable for our experiments. This selection was made by taking preliminary diffraction figures, and the profitable specimens were chosen for further experiments.

Experimental Results.

I. Bismuth

(i) Specimen-A. A piece of Specimen-A_1 (0·7 mm. in diameter), with which the experiment was first performed, was pasted on a sheet of paper, so that its lamellar face became parallel to the surface of the paper. When this lamellar face, which coincided with the surface of

1 H. Hirata & H. Komatsubara: These Memoirs, **10**, 85 (1926); or Z. S. f. Anorg. u. Allgem. Chem., **158**, 137 (1926).

the paper, was set perpendicular to the incident beam, then the diffraction figure reproduced in Fig. 11, Plate II, was usually obtained on the photographic plate.

In this figure, the prominent part or "intensity maxima", consists of a number of concentric circular rings and several radiating bands which have many intense spots on them. Thus we can conclude, from Fig. 11, that the Specimen-A_1 is partly composed of a fibrous structure, but considerable portion of it consists perhaps of an irregular aggregation of the micro-crystals.

Fig. 12, Plate II, is the diffraction figure taken with the Specimen-A_2, in a similar way as Fig. 11, plate II. In this case a piece of the lamellar specimens (0·8–1·2 mm. in diameter) was used. The diffraction pattern obtained, as can be seen in Fig. 12, Plate II, consists of a number of radiating bands; but no concentric circular rings can be detected. The absence of concentric circular rings in this case shows us without doubt, that the growth of fibrous structure is complete in Specimen-A_2: i. e., the specimen does not contain any considerable irregular aggregation of the micro-crystals, but that it is mostly made up of the fibrous crystalline arrangements.

Next, the writer extended his investigation to Specimen-A_3. The specimens belonging to this group came to appear mostly in an acicular form; and a few lamellar mixtures could also be found among these aciculae. With a lamellar fragment of Specimen-A_3, the interference figure was taken in a similar way as Figs. 11 and 12, Plate II; while to take the interference figure with an acicular specimen, the acicular axis was placed perpendicularly to the direction of the incident ray. The diffraction figure obtained in the former case, (not reproduced) was of the pattern consisting not only of a number of radiating bands, but also of an irregular assemblage of many Laue's spots; while, in the latter case, we obtained the figure reproduced in Fig. 13, Plate II. The prominent part of this figure consists of a set of Laue's spots, which seem to be produced by a single crystal, as will be considered later.

Thus we may conclude, from the presence of Laue's spots in both figures above-mentioned, that Specimen-A_3 is composed of crystals of considerable dimensions. Especially, in the acicular specimen, which gave rise to Fig. 13, Plate II, the growth of the crystal of bismuth is so complete that the trace of fibrous or irregular aggregations of the micro-crystals can no more be detectable.

Here, it must be remarked that the foregoing statement is rather a general, or so to speak, a statistical one, obtained from many specimens

belonging to every sub-class. Here and there occasionally a few exceptions were detected: e. g., some of the specimens belonging to Specimen-A_1 (in the ratio of 1 to 4) gave rise to a diffraction figure which was essentially the same as that obtained with Specimen-A_2. The prominent part of this figure consisted of several radiating bands of the same angular distribution as that in Fig.12, Plate II, without any concentric circular rings.

Conversely to the case above stated, the same diffraction figure Fig. 14, Plate II, as with Specimen-A_1 was sometimes obtained with Specimen-A_2 (in the ratio of 1 to 4).

It was confirmed, however, that such an interchange of the corresponding figures between two different specimens occurred only when their suffix numbers differed by one; i.e., the two specimens which interchanged their corresponding diffraction figures, were always those deposited under the nearest conditions. From this fact, we may suppose that the exceptions above stated are due probably to some accidental causes, such as the variation of the local current density.

The argument which has hitherto been advanced with respect to Specimen-A, leads us to the following conclusions:-

When the current density and the concentration of the electrolyte are comparatively large, the micro-crystals of bismuth have no remarkable tendency to deposit themselves in a fibrous form. But, this tendency becomes the more remarkable with a smaller current density and smaller concentration of the electrolyte, and a perfect fibrous arrangement is realizable under such conditions as will produce Specimen-A_2.

In an extreme case, when the current density and the concentration of the electrolyte are so small as to produce Specimen-A_3, the electrodeposit tends to form single crystals of considerable dimensions.

(ii) Specimen B. The specimens belonging to this group, as already stated, were of apparently non-metallic amorphism with an appearance like platinum black. Among the specimens of this category, Specimens B_1, B_2, and B_3 came to appear in a very brittle cloddy form, while Specimen B_4 was of a lamella deposited on the surface of the cathode.

All of these specimens have no proper micro-structure of metallic bismuth. Consequently, it was questionable whether they were composed of metallic bismuth, or of its compound.

Now, to investigate the crystalline structure of those specimens, the diffraction figures were taken in two different ways. With a cloddy specimen such as Specimens B_1, B_2, and B_3, a diffraction figure was taken by transmitting the incident beam of X-rays to a small clod of

the specimen, which had been pasted on a sheet of paper. Next, with Specimen-B_4, which was a lamellar aggregation of numerous fine grains, the writer investigaetd the interference phenomena obtained in the following two orientations of the sample: one when the surface of the lamella was set perpendicular to the direction of the incident beam, and the other when it was rotated by about 20° around an axis perpendicular to the direction of the incident beam. In this way, it should be possible to detect regular structures, if any, in the specimen.

From these results of the investigation, it became clear that the same diffraction figure is obtainable with all the specimens belonging to Specimen-B. In this figure, the prominent part of the diffraction-pattern consisted of a number of concentric circular rings as shown in Fig. 17, Plate III, which was produced by the normal incidence of X-ray-beam on the lamellar surface of Specimen B_4. It will be shown later that the radii of these concentric circular rings agree fairly well with the results of calculation, carried out from the experimental data of metallic bismuth given by James[1] and Ogg,[2] and from the wavelength of the K_α radiation of molybdenum.

As a consequence of such calculation, it was seen that the concentric rings $I'_{1,2}$, II', $III'_{1,2}$, I_1'', I_2'', II'', IV_1', and I_2''' in Fig.17, Plate III were produced by the prominnt atomic planes of the indices[3] $(111)_I$ and $(\bar{1}11)_I$, $(100)_I$, $(110)_I$ and $(\bar{1}10)_I$, $(111)_{II}$, $(\bar{1}11)_{II}$, $(100)_{II}$, $(211)_I$, and $(\bar{1}10)_{III}$ respectively. Here, it must be understood that the numerical suffixes used in the symbols $(\quad)_I$, $(\quad)_{II}$, and $(\quad)_{III}$ denote the order of the spectrum.

From these facts, it can be inferred that the so called amorphous deposits under consideration, or some part of them at least, are not amorphous, but composed mainly of the irregular aggregation of the micro-crystals of metallic bismuth. Moreover, as was stated before, the diffraction-figure was essentially the same as Fig.17, Plate III, even when Specimen-B_4 was tilted from its normal position against the incident beam. This shows that the micro-crystals in the specimen are irregularly orientated with respect to any direction.

---

1 Phil. Mag., **42**, 193 (1921).

2 Phil. Mag., **42**, 163 (1921).

3 To represent the family of atomic planes in bismuth or antimony, the notation is used in the same way as by James & Tunstall.[4]

4 Phil. Mag.. **40**, 233 (1920)

II. Antimony.

(i) Specimen A. Fig.15, Plate III is the diffraction figure taken with a piece of Specimen-A_2. To obtain this figure, the face of this lamellar specimen was set perpendicular to the incident beam, as was done with a lamellar specimen of bismuth.

The prominent part of Fig.15 in Plate III consists of a set of Debye-Hull's rings I_2'', II'', IV_1', I_1''', III_1'' and II''', which were found, from the results of calculation, described later, to be produced by the reflection from the prominent atomic planes of the indices $(11\bar{1})_{II}$, $(100)_{II}$, $(211)_I$, $(111)_{III}$, $(110)_{II}$, and $(100)_{III}$ respectively.

It can also be expected that the rings corresponding to $(\bar{1}11)_I$, $(100)_I$, $(110)_I$ and $(\bar{1}10)_I$ would come to appear in the figure. But they are considered to fall inside the broad central spot, because their radii are smaller than that of the central spot. No clear evidence of the fibrous structure was detected in this case, as in the case of Bi.

Specimen B: As Specimen B_4 of Bi, Specimen B_1 of Sb was also a black cloddy lamella formed on the cathode. To examine this specimen, the writer took the diffraction figures in two orientations of the sample, as was the case with Specimen B_4 of Bi: i.e., one when its lamellar face was set perpendicular to the direction of the incident beam, and the other when it was rotated by about 20° around an axis perpendicular to the direction of the incident beam. Fig.16, Plate III is the diffraction figure obtained in the former orientation. The prominent part of this figure consists, as with Specimen B of Bi, of a number of concentric circular rings. The same figure as Fig.16 Plate III was also obtained in the latter orientation.

Consequently, we may conclude that the majority of the micro-crystals in Specimen B_1 of Sb is irregularly orientated with respect to any direction.

The same calculation as with Specimen A of Sb applies well to the present instance. As its results, it became clear that the rings II', $III'_{1,2}$, I_1'', I_2'', II'', IV_1', I_1''' and I_2''' in Fig.16 Plate III were due to the reflections of the X-rays from the prominent atomic planes of the indices $(100)_I$, $(110)_I$ and $(\bar{1}10)_I$, $(111)_{II}$, $(\bar{1}11)_{II}$, $(100)_{II}$, $(211)_I$, $(111)_{III}$, and $(\bar{1}11)_{III}$ respectively.

The facts so much as were confirmed, lead us to the same conclusion as in the case of the Specimen B of Bi: i.e., the most part, if not the whole, of the apparently amorphous Specimen B of Sb, is not amorphous, but composed of an irregular aggregation of the micro-

crystals of antimony.

Discussion of the Experimentat Results. In the preceding chapter, rather qualitative arguments were advanced with respect to the crystalline structure of each specimen. The further arguments we now attempt to make in this chapter, aim at the quantitative explanation of our experimental facts. In the first place, the indices of the atomic planes which gave rise to the intense spots on the radiating bands and to the Debye-Hull's rings observed, will be determind by calculation. Secondly will be investigated what direction of the fibrous axis would produce the angular distribution of radiating bands, as was observed with Specimen-A_2 of Bi. The last part of the arguments will deal with the mechanism of the formation of Laue's Figure as was observed with some specimens belonging to Specimen-A_3 of Bi.

Now, before entering into detail, it would be well to find out the formulae from which the numerical values of an angle between two atomic planes and the spacing of each one of these planes in the crystal are derived. By making use of these numerical values, Yoshida's "globe and spherical scale"[1] which facilitates the troublesome calculations, can be made available to our present investigation.

Fig. 1 Antimony Type Space-Lattice

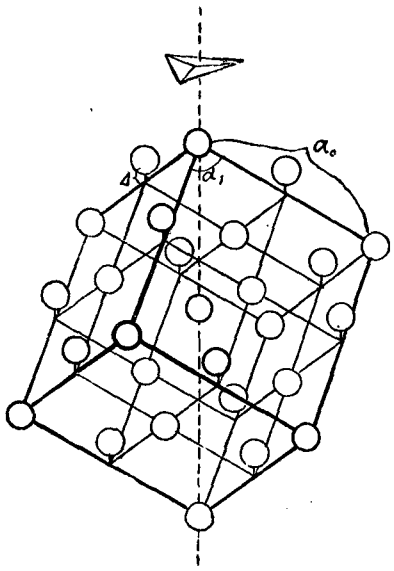

From the researches of James,[2,4] Tunstall[2], Ogg[3] and others,[5] it is known that the crystals of both metals under consideration, as are represented diagrammatically in Fig.1, consist of two interpenetrating face-centred rhombohedral lattices, which have a trigonal axis in common. Moreover it is already known that the rhombohedral angles a_1 of bismuth and antimony crystals are 87°34′ and 86° 58′ respectively. While, two rhombohedral lattices which form the bismuth or antimony crystal are considered to

1 U. Yoshida: Japanese. J. Phys., 4, 133 (1927).
2 Loc. cit.
3 Loc. cit.
4 Loc. cit.
5 L. W. Mc Keehan: Journ. Franklin Institute, Jan., (1923).

be displaced to each other by $\triangle=0.027\ t_0$ and $\triangle=0.04\ t_0$ respectively, along the common trigonal axis, where t_0 is the length of this common trigonal axis of the unit cell. If we represent the length of the rhombohedral edge of the unit cell by a_0, it amounts to 6.20×10^{-8} cm. in antimony. As to the numerical value of a_0 in bismuth, James and others gave 6.56×10^{-8} cm., while, according to Ogg, it amount to 6.52×10^{-8} cm. Thus, let us use their mean value 6.53×10^{-8} cm. in our further calculation.

Now, let us take the three rhombohedral edges which incline with the angle α_1 with each other as the axes of an oblique co-ordinate system, and the corner atom situated at the intersecting point of these axis as the origin. If we temporarily suppose that the crystals are of the simple rhombohedral lattice, then the equations of the atomic planes with the indices h k l and h′ k′ l′ will respectively be given by

$$\left.\begin{aligned} hx+ky+lz&=a_0 \qquad (1a)\\ h'x+k'y+l'z&=a_0 \qquad (1b)\end{aligned}\right\}$$

Now, let ξ, η, ζ, and ξ', η', ζ' be the two sets of the angles between the co-ordinate axes and the normals of these two atomic planes respectively, then the perpendicular distances d_{hkl} and $d_{h'k'l'}$ from the origin to these planes should be expressed respectively by

$$\frac{\mathrm{Cos}\ \xi}{h}=\frac{\mathrm{Cos}\ \eta}{k}=\frac{\mathrm{Cos}\ \zeta}{l}=\frac{d_{hkl}}{a_0}$$

$$\frac{\mathrm{Cos}\ \xi'}{h'}=\frac{\mathrm{Cos}\ \eta'}{k'}=\frac{\mathrm{Cos}\ \zeta'}{l'}=\frac{d_{h'k'l'}}{a_0}$$

$\mathrm{Cos}\,\xi$, $\mathrm{Cos}\,\eta$, $\mathrm{Cos}\,\zeta$ and $\mathrm{Cos}\,\xi'$, $\mathrm{Cos}\,\eta'$, $\mathrm{Cos}\,\zeta'$ in the above expressions being respectively the direction cosines of the same straight line, the following relations (3) and (4) should hold good in the present case.

$$\begin{vmatrix} 1 & \mathrm{Cos}\,\alpha_1 & \mathrm{Cos}\,\alpha_1 & \mathrm{Cos}\,\xi\\ \mathrm{Cos}\,\alpha_1 & 1 & \mathrm{Cos}\,\alpha_1 & \mathrm{Cos}\,\eta\\ \mathrm{Cos}\,\alpha_1 & \mathrm{Cos}\,\alpha_1 & 1 & \mathrm{Cos}\,\zeta\\ \mathrm{Cos}\,\xi & \mathrm{Cos}\,\eta & \mathrm{Cos}\,\zeta & 1 \end{vmatrix}=0 \qquad (3)$$

$$\begin{vmatrix} 1 & \mathrm{Cos}\,\alpha_1 & \mathrm{Cos}\,\alpha_1 & \mathrm{Cos}\,\xi'\\ \mathrm{Cos}\,\alpha_1 & 1 & \mathrm{Cos}\,\alpha_1 & \mathrm{Cos}\,\eta'\\ \mathrm{Cos}\,\alpha_1 & \mathrm{Cos}\,\alpha_1 & 1 & \mathrm{Cos}\,\zeta'\\ \mathrm{Cos}\,\xi' & \mathrm{Cos}\,\eta' & \mathrm{Cos}\,\zeta' & 1 \end{vmatrix}=0 \qquad (4)$$

Moreover, the angle β_1 between the two atomic planes (1_a) and (1_b) should be given by

$$\begin{vmatrix} 1 & \cos a_1 & \cos a_1 & \cos \xi' \\ \cos a_1 & 1 & \cos a_1 & \cos \eta' \\ \cos a_1 & \cos a_1 & 1 & \cos \zeta' \\ \cos \xi' & \cos \eta' & \cos \zeta' & \cos \beta_1 \end{vmatrix} = 0 \qquad (5)$$

Consequently, from (2), (3), (4). and from the above expression (5), we get

$$\cos \beta_1 = \frac{\Sigma hh' \sin \alpha_1 + \Sigma kl' (\cos^2 \alpha_1 - \cos \alpha_1)}{\sqrt{\{\Sigma h^2 \sin^2 \alpha_1 + 2\Sigma kl (\cos^2 \alpha_1 - \cos \alpha_1)\}\{\Sigma h'^2 \sin^2 \alpha_1 + 2\Sigma k'l' (\cos^2 \alpha_1 - \cos \alpha_1)\}}} \qquad (6)$$

$$\left.\begin{aligned} d_{hkl} &= \frac{a_0 \sqrt{1 + 2\cos^3 a_1 - 3\cos^2 a_1}}{\sqrt{\Sigma h^2 \sin^2 a_1 + 2\Sigma kl (\cos^2 a_1 - \cos a_1)}} \\ d_{h'k'l'} &= \frac{a_0 \sqrt{1 + 2\cos^3 a_1 - 3\cos^2 a_1}}{\sqrt{\Sigma h'^2 \sin^2 a_1 + 2\Sigma k'l' (\cos^2 a_1 - \cos a_1)}} \end{aligned}\right\} \qquad (7)$$

As was stated before, the above expressions (6) and (7) represent respectively the angle between the normals of two atomic planes and the spacings of these planes in a simple rhombohedral lattice. These expressions can easily be modified as to be applicable to a face-centred rhombohedral lattice, as is the case in bismuth or antimony. In the following articles, the experimental results will be compared with the consequence of calculations which are founded on the above two expressions.

The angles between any crystal axis and the normals to various atomic planes of the crystals may be calculated similarly as above.

(i) On the Formation of Debye-Hull's Rings:

The expression (7) represents the spacing between two consecutive atomic planes having the indices $h\ k\ l$ in a simple rhombohedral lattice. Thus, if we modify the expression (7) so that it be applicable to a face-centred rhombohedral lattice, and substitute the proper numerical values for a_1 and a_0, the spacing of each atomic plane in bismuth or antimony crystal should immediately be found.

In each of the first columns of Tables 1 and 2, the indices of the prominent atomic planes of bismuth and antimony are represented. The numerical values of the corresponding spacing d, thus calculated from expression (7), are given in the second columns of the same Tables.

From these numerical values of d, the radii of Debye-Hull's rings on the photographic plate will be calculated. For this purpose a calculation was carried out, by making use of the following two well known relations :—

$$2a \text{ Sin } \theta = n\lambda \qquad (8)$$

$$L \text{ Tan } 2\theta = r \qquad (9)$$

where n is a positive integer representing the order of the spectrum, θ the glancing angle of the incident X-ray, λ the wavelength of the incident X-rays, and L the distance of the photographic plate from the specimen. The value of L was 3.2 cm. in the present experiment.

The values of γ thus calculated are given in the fourth columns of

Table 1 *Bi*

Calculated Values						Observed Values			
Indices of the Reflecting Planes			d in 10^{-8} cm.	n	r in. cm.	r in cm. Fig. 11	r in cm. Fig. 14	r in cm. Fig. 17	No. of Rings
1	1	1	3.934	1 2 3	0.58 1.22 1.95	1.23	1.23	1.23	— I_1'' —
1	1	$\bar{1}$	3.719	1 2 3	0.62 1.29 2.10	1.29 2.10	1.31	1.28 2.10	— I_2'' I_2'''
1	1	0	2.357	1 2 3	1.00 2.25 4.36	*	0.97	*	III_1' — —
1	$\bar{1}$	0	2.264	1 2 3	1.04 2.37 4.77	*	1.05	* 2.39	III_2' III_2'' —
1	0	0	3.265	1 2 3	0.69 1.50 2.51	* 1.50	* 1.50	* 1.49	— II'' —
2	1	1	1.381	1	1.83		1.80	1.80	IV_1
2	1	$\bar{1}$	1.341	1	1.89				—
$\bar{2}$	1	1	1.306	1	1.96				—

Table 2 *Sb*

Calculated Values						Observed Values		
Indices of the Reflecting Planes			d in 10^{-8} cm.	n	r in cm.	r in cm. Fig. 15	r in cm. Fig. 16	No. of Rings
1	1	1	3.770	1	0.61			—
				2	1.27		1.25	I_1''
				3	2.06	2.06		I_1'''
1	1	$\bar{1}$	3.517	1	0.65			—
				2	1.38	1.38	1.41	I_2''
				3	2.26		2.26	I_2'''
1	1	0	2.299	1	1.05	*	*	—
				2	2.40	2.39		III_1''
				3	4.85			—
1	$\bar{1}$	0	2.135	1	1.11	*	1.11	III_2'
				2	2.58			—
				3	5.50			—
1	0	0	3.096	1	0.75	*	0.75	II'
				2	1.60	1.62	1.65	II''
				3	2.71	2.79		II'''
2	1	1	1.321	1	1.94	1.92	1.94	IV_1'
2	1	$\bar{1}$	1.254	1	2.07			—
$\bar{2}$	1	1	1.223	1	2.14			—

Tables 1 and 2. To calculate these numerical values of γ, we have assigned to λ the value of the wavelength of the K_α line of molybdenum. Though it may be possible that the K_β line of molybdenum will also appear, yet as the intensity of this line is very feeble compared with that of the K_α line, the latter line has only been taken to our consideration. For the value of the wavelength of the K_α line, we have given the mean value of the $K_{\alpha 1}$ and $K_{\alpha 2}$ lines, which is equal to $\lambda_\alpha = 709.73 \times 10^{-11}$ cms.

The numerical values of γ can also be obtained by measuring the radii of the rings in the figures. These observed values of γ are represented in the fifth, sixth and seventh columns of Table 1, and in the fifth and sixth columns of Table 2. The Roman numerals in the last columns of Table 1 and 2 denote the numbers of the rings from which these numerical values of γ are measured.

As was to be expected, each one of these observed values of γ agrees fairly well with one of the calculated values in the fourth column of the Tables.

In these two Tables, the rings marked with an asterisk were expected to be so intense, that they would be detectable in the figures. But, this did not come out sight, owing to their radii being smaller than that of the broad central spot.

As the consequence of the foregoing arguments, we may legitimately assign the indices of the atomic planes and the order of the spectra as given in the first and third columns to each concentric ring which is represented in the last columns of the Tables.

In the Tables 1 and 2, the indices of the atomic planes and the order of the radiation were attributed to each Debye-Hull's ring, which was obtained with the Specimens of *Bi* and *Sb*. Such a correspondency between the indices of the atomic plane and the concentric rings was found to exist not only with respect to Figs. 11, 14, 15, 16, and 17, but to all the diffraction figures obtained in this experiment. Consequently, it seems to be legitimate to consider that each concentric ring in these figures was produced by the reflection of a prominent atomic plane in the bismuth or antimony crystals.

(ii) On the Formation of the Radiating Bands:

Next, let us determine the direction of the fibrous axis which will produce an angular distribution of radiating bands as in Figs. 12 and 14, Plate II. For this purpose the following relation was used: —

$$\mathrm{Cos}\,\beta=\mathrm{Cos}\,\gamma\,\mathrm{Cos}\,\alpha+\mathrm{Sin}\,\gamma\,\mathrm{Sin}\,\alpha\,\mathrm{Cos}\,\varphi \qquad (10)$$

where α is the angle between the incident ray and the fibrous axis of the crystals, β the angle between the normal of a certain reflecting plane and the fibrous axis of the crystals, $\gamma=\frac{\pi}{2}-\theta$ the angle between the incident ray and the normal of the reflectiong plane, and φ the azimuth of a point on a radiating band measured on the photographic plate from the line of intersection of the photographic plate with the plane containing the incident X-rays and the fibre, by taking the central spot as the pole.

From the above relation (10) and equation (9), each radiating band will be traced out, for definite values of α and β, by giving various values to γ and by finding the numerical relations between φ and γ. Especially when $\alpha=\frac{\pi}{2}$ the radiating bands become nearly straight in the vicinity of the central spot, and the values of φ will be nearly equal to β. Thus, if the value of β is found by measuring the angles between

Table 3. The Numerical Values of β_1

k k l	1 0 0	0 1 0	0 0 1	1 1 0	1 0 1	0 1 1	1 1 0	1 0 $\bar{1}$	0 $\bar{1}$ 1	1 1 1	$\bar{1}$ 1 1	1 $\bar{1}$ 1	1 1 $\bar{1}$	2 1 1	$\bar{2}$ 1 1	2 $\bar{1}$ 1	2 1 $\bar{1}$	1 2 1	$\bar{1}$ 2 1	1 $\bar{2}$ 1	1 2 $\bar{1}$	1 1 2	$\bar{1}$ 1 2	1 $\bar{1}$ 2	1 1 $\bar{2}$
1 0 0	0°	87° 40′	87° 40′	46° 10′	46° 10′	86° 37′	44° 53′	44° 53′	90°	56° 24′	51° 58′	55° 17′	55° 17′	33° 14′	33° 36′	35° 49′	35° 49′	68° 13′	62° 56′	65° 24′	67° 7′	68° 13′	62° 56′	67° 7′	65° 24′
0 1 0	87° 40′	0°	87° 40′	46° 10′	86° 37′	46° 10′	44° 53′	90°	44° 53′	56° 24′	55° 17′	51° 58′	55° 17′	67° 58′	68° 13′	62° 56′	67° 7′	33° 14′	35° 49′	33° 36′	35° 49′	68° 13′	67° 7′	62° 56′	65° 24′
0 0 1	87° 40′	87° 40′	0°	86° 37′	46° 10′	86° 37′	90°	44° 53′	44° 53′	56° 24′	55° 17′	55° 17′	51° 58′	67° 58′	68° 13′	67° 7′	62° 56′	68° 13′	67° 7′	65° 24′	62° 56′	33° 14′	35° 49′	35° 49′	33° 36′
1 1 0	46° 10′	46° 10′	86° 37′	0°	62° 47′	62° 47′	90°	55° 40′	55° 40′	36° 57′	88° 5′	88° 5′	34° 40′	31° 20′	72° 30′	75° 7′	29° 59′	31° 20′	75° 7′	72° 30′	29° 59′	57° 36′	87° 16′	87° 16′	53° 3′
1 0 1	46° 10′	86° 37′	46° 10′	62° 47′	0°	62° 47′	55° 40′	90°	55° 40′	36° 57′	88° 5′	34° 40′	88° 5′	31° 20′	72° 30′	29° 59′	75° 7′	57° 36′	87° 16′	53° 3′	87° 16′	31° 20′	75° 7′	29° 59′	72° 30′
0 1 1	86° 37′	46° 10′	46° 10′	62° 47′	62° 47′	0°	55° 40′	55° 40′	90°	36° 57′	34° 40′	88° 5′	88° 5′	57° 36′	53° 3′	87° 16′	87° 16′	31° 20′	29° 59′	72° 30′	75° 7′	31° 20′	29° 69′	75° 7′	72° 30′
1 $\bar{1}$ 0	44° 53′	44° 53′	90°	90°	55° 40′	55° 40′	0°	60°	60°	90°	34° 43′	34° 43′	90°	73° 40′	29° 59′	29° 37′	72° 59′	73° 40′	29° 37′	29° 59′	72° 59′	90°	54° 11′	54° 11′	90°
1 0 $\bar{1}$	44° 53′	90°	44° 53′	55° 40′	90°	55° 40′	60°	0°	60°	90°	34° 43′	90°	34° 43′	73° 40′	29° 59′	72° 59′	29° 37′	90°	54° 11′	90°	54° 11′	73° 40′	29° 37′	72° 59′	29° 59′
0 $\bar{1}$ 1	90°	44° 53′	44° 53′	55° 40′	55° 40′	90°	60°	60°	0°	90°	90°	34° 43′	34° 43′	90°	90°	54° 11′	54° 11′	73° 40′	72° 59′	29° 59′	29° 37′	73° 40′	72° 59′	29° 37′	29° 59′
1 1 1	56° 24′	56° 24′	56° 24′	36° 57′	36° 57′	36° 57′	90°	90°	90°	0°	71° 43′	71° 43′	71° 43′	20° 37′	90°	63° 20′	63° 20′	20° 37′	63° 20′	90°	63° 20′	20° 37′	63° 20′	63° 20′	90°
$\bar{1}$ 1 1	51° 58′	55° 17′	55° 17′	88° 5′	88° 5′	34° 40′	34° 43′	34° 43′	90°	71° 43′	0°	69° 27′	69° 27′	87° 45′	18° 24′	60° 2′	60° 2′	62° 28′	19° 5′	61° 41′	88° 56′	62° 28′	19° 5′	88° 56′	61° 41′
1 $\bar{1}$ 1	55° 17′	51° 58′	55° 17′	88° 5′	34° 40′	88° 5′	34° 43′	90°	34° 43′	71° 43′	69° 27′	0°	69° 27′	62° 28′	61° 41′	19° 5′	88° 56′	87° 45′	60° 2′	18° 24′	60° 2′	62° 28′	88° 56′	19° 5′	61° 41′
1 1 $\bar{1}$	55° 17′	55° 17′	51° 58′	34° 40′	88° 5′	88° 5′	90°	34° 43′	34° 43′	71° 43′	69° 27′	69° 27′	0°	62° 28′	61° 41′	88° 56′	19° 5′	62° 28′	88° 56′	61° 41′	19° 5′	87° 45′	60° 2′	60° 2′	18° 24′
2 1 1	33° 14′	68° 13′	68° 13′	31° 20′	31° 20′	57° 36′	73° 40′	73° 40′	90°	20° 37′	87° 45′	62° 28′	62° 28′	0°	69° 23′	48° 52′	48° 52′	35° 31′	82° 58′	79° 51′	61° 21′	35° 31′	82° 58′	61° 21′	79° 51′
$\bar{2}$ 1 1	33° 36′	65° 24′	65° 24′	72° 30′	72° 30′	53° 3′	29° 59′	29° 59′	90°	90°	18° 24′	61° 41′	61° 41′	69° 23′	0°	47° 31′	47° 31′	79° 51′	32° 24′	60°	80° 17′	79° 51′	32° 24′	80° 17′	60°
2 $\bar{1}$ 1	35° 49′	62° 56′	67° 7′	75° 7′	29° 59′	87° 16′	29° 37′	72° 59′	54° 11′	63° 20′	60° 2′	19° 5′	88° 56′	48° 52′	47° 31′	0°	71° 37′	82° 58′	57° 18′	32° 24′	80° 4′	61° 21′	80° 4′	34° 1′	80° 17′
2 1 $\bar{1}$	35° 49′	67° 7′	62° 56′	29° 59′	75° 7′	87° 16′	72° 59′	29° 57′	54° 11′	63° 20′	60° 2′	88° 56′	19° 5′	48° 52′	47° 31′	71° 37′	0°	61° 21′	80° 4′	80° 17′	34° 1′	82° 58′	57° 18′	80° 4′	32° 24′
1 2 1	68° 13′	33° 14′	68° 13′	31° 20′	57° 36′	31° 20′	73° 40′	90°	73° 40′	20° 37′	62° 28′	87° 45′	62° 28′	35° 31′	79° 51′	82° 58′	61° 21′	0°	48° 52′	69° 23′	48° 52′	35° 31′	61° 21′	82° 58′	79° 51′
$\bar{1}$ 2 1	62° 56′	35° 49′	67° 7′	75° 7′	87° 16′	29° 59′	29° 37′	54° 11′	72° 59′	63° 20′	19° 5′	60° 2′	88° 56′	82° 58′	32° 24′	57° 18′	80° 4′	48° 52′	0°	47° 31′	71° 37′	61° 21′	34° 1′	80° 17′	80° 4′
1 $\bar{2}$ 1	65° 24′	33° 36′	65° 24′	72° 30′	53° 3′	72° 30′	29° 59′	90°	29° 59′	90°	61° 41′	18° 24′	61° 41′	79° 51′	60°	32° 24′	80° 17′	63° 29′	47° 31′	0°	47° 31′	79° 51′	80° 17′	32° 24′	60°
1 2 $\bar{1}$	67° 7′	35° 49′	62° 56′	29° 59′	87° 16′	75° 7′	72° 59′	54° 11′	29° 37′	63° 20′	88° 56′	60° 2′	19° 5′	61° 21′	80° 17′	80° 4′	34° 1′	48° 52′	71° 37′	47° 31′	0°	82° 58′	80° 4′	57° 18′	32° 24′
1 1 2	68° 13′	68° 13′	33° 14′	57° 36′	31° 20′	31° 20′	90°	73° 40′	73° 40′	20° 37′	62° 28′	62° 28′	87° 45′	35° 31′	79° 51′	61° 21′	82° 58′	35° 31′	61° 21′	79° 51′	82° 58′	0°	48° 52′	48° 52′	69° 23′
$\bar{1}$ 1 2	62° 56′	67° 7′	35° 49′	87° 16′	75° 7′	29° 59′	54° 11′	29° 37′	72° 59′	63° 20′	19° 5′	88° 56′	63° 2′	82° 58′	32° 24′	83° 4′	57° 18′	61° 21′	34° 1′	80° 17′	80° 4′	48° 52′	0°	71° 37′	47° 31′
1 $\bar{1}$ 2	67° 7′	62° 56′	35° 49′	87° 16′	29° 59′	75° 7′	54° 11′	72° 59′	29° 37′	63° 20′	88° 56′	19° 5′	60° 2′	61° 21′	80° 17′	32° 24′	80° 4′	82° 58′	80° 4′	32° 24′	57° 18′	48° 52′	71° 37′	0°	47° 31′
1 1 $\bar{2}$	65° 24′	65° 24′	33° 36′	53° 3′	72° 30′	72° 30′	90°	29° 59′	29° 59′	90°	61° 41′	61° 41′	18° 24′	79° 51′	60°	80° 17′	32° 24′	79° 51′	80° 17′	60°	32° 24′	69° 23′	47° 31′	47° 31′	0°

the bands, the axis of the crystal arranged in the direction of the axis of the fibre will be known immediately.

In Figs. 12 and 14, Plate II, all the radiating bands are nearly straight. This indicates that the axis of the fibre was nearly perpendicular to the incident beam of the X-rays, and is in a direction nearly parallel to the lamellar surface of the specimens in these cases. Thus from the relation stated above the value of φ may be taken to be equal to that of β in these cases.

Now let us provisionally suppose that the normal to one of the atomic planes in bismuth-crystals is arranged parallel to the direction of the fibrous axis. If our consideration be correct, the calculated values of β_1, whice represent the angles between the normals to various atomic planes and the direction of the fibrous axis, should agree well with the numerical values of β measured in the vicinity of the central spot on the photographic plates.

Table 3 represents the numerical values of β_1, obtained from the expression (6). All these numerical values of β_1, were confirmed to be correct by using the Yoshida globe and sphericals scale[1].

Thus the fundamental problem is to find out the direction, on the photographic plate, which is parallel to the direction of the fibrous axis. This was accomplished by trial by taking successively the various directions on the photographic plate as the direction of the fibrous axis and by examining the agreement between the observed values of β and the calculated values of β_1 for various atomic planes by taking a certain atomic plane as a reference plane.

With respect to Fig. 12, Plate II, the direction represented by an arrow in that figure was found, in the manner above stated, to be the best one for the direction parallel to the fibrous axis of the specimen. The values of β for various radiating bands in Fig. 12, Plate II, which were measured from the direction represented by the arrow, are given in the third, fourth, fifth, and sixth columns of Table 4. The value of β for each radiating band the number of which is denoted in the seventh column of Table, was measured each quadrant of the figure.

Here it can be noticed that these observed values of β are nearly equal to the calculated values of β_1, in the vertical rows corresponding to the indices 2 1 1, 1 2 1 and 1 1 2 in Table 3. Thus it will not be unnatural to consider that the atomic planes of the indices (2 1 1) are

---

1 Loc. cit.

Table 4.

Calculated Values		Observed Values					
Indices of Pls. h k l	β_2	β 1st Quadrant	β 2nd Quadrant	β 3rd Quadrant	β 4th Quadrant	No. of Rad Bds.	Indices of Family of Pls.
1 1 1	18° 20′	19°	18°	19°	18°	I_1	(1 1 1)
1 1 0 1 0 1	31° 28′	—	—	31°	—	III_1	(1 1 0)
1 0 0	38° 2′	38°	38°	38°	38°	II	(1 0 0)
0 1 1	55° 21′	—	—	—	—	III_1	(1 1 0)
1 $\bar{1}$ 1 1 1 $\bar{1}$	63° 21′	63°	63°	63°	63°	I_2	(1 1 $\bar{1}$)
0 1 0 0 0 1	66° 48′	66°	66°	—	66°	II	(1 0 0)
1 1 0 1 0 $\bar{1}$	74° 9′	74°	74°	76°	75°	III_2	(1 1 0)
0 1 1 1 1 1	90°	88°	90°	90°	92°	$I_2 III_2$	(1 1 $\bar{1}$) (1 $\bar{1}$ 0)

arranged nearly, though not exactly, parallel to the direction of the fibrous axis in this case.

Next, in expressing the direction of the crystal, which is arranged parallel to the direction of the axis of the fibre, it is more natural to take a crystallographic axis than to take the normal of an atomic plane of the crystal. These two directions are slightly different in the case of bismuth and antimony. As the angle between the crystallographic axis [2 1 1] and the normal to the corresponding atomic plane 2 1 1 is only 2° 27′ in the case of the bismuth-crystal, the writer preferred the crystallographic axis [2 1 1] as the axis of the fibre.

The values of β_2 calculated and tabulated in Table 4 are the angles between the crystallographic axis [2 1 1] and the normals to various atomic planes, whose indices are given in the first column of the same table. A fair agreement between the values observed for β and those calculated for β_2 will be seen in the table.

In Fig. 12, Plate II, we can detect the appearance of the intense spots on some of the radiating bands. These intense spot are certainly caused by the reflections of the K_α radiation of molybdenum from various

atomic planes. The indices of each one of these atomic planes were founded from the value of the spacing between two consecutive atomic planes, which was calcutated from the wavelength of the K_α line of molybdenum and the distance of the corresponding intense spot from the centre of the central spot. The indices thus determined experimentally are given in the last column of Table 4, and they are in fair accordance with those given in the first column of that table.

Next, as to the problem whether or not another crystallographic axis may be taken as the axis of the fibre, it was confirmed also by means of the globe and spherical scale devised by U. Yoshida that no other axis than [2 1 1] could account for the distribution of the radiating bands in Fig. 12, Plate II.

The full lines in the annexed Fig. 2 represent diagrammatically the prominent radiating bands, traced out with the calculated values given in the second column of Table 4; and the short lines crossing these radiating bands express the calculated positions of the impression of the K_α line of *Mo* on the photographic plate. The shaded part in the same figure is the copy of the diffraction pattern in Fig. 12, Plate II.

Fig. 2.

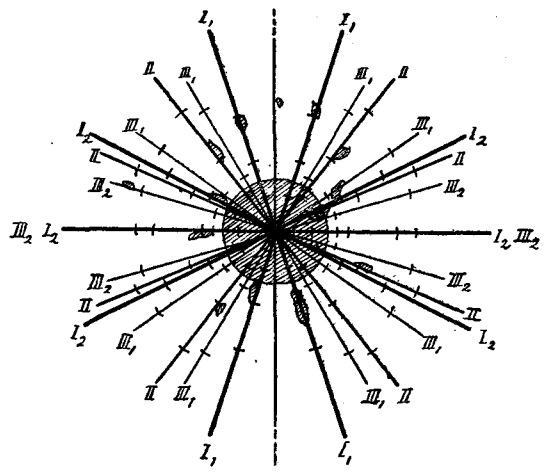

As may be seen from the figure, not only with respect to the angular distribution of the radiating bands, but also with respect to the positions of the intense spots, the agreement between the calculated curves and the obrerved ones is rather satisfactory. Moreover, this agreement was

found to hold good also not only in Fig. 12 but in all the figures consisting of several radiating bands, as Figs. 11 and 14. The arrow in these figures represents the direction of the fibrous axis.

Thus our consideration having been confirmed as above, we may legitimately conclude that the micro-crystals of bismuth have a tendency to deposit themselves in a fibrous from with the crystal-axis [2 1 1] arranged parallel to the direction of the fibrous axis.

Next, to confirm the above consideration still further, the writer investigated the interference phenomena obtained in two orientations of the samples, one when it was rotated 22° around the direction parallel to the axis of the fibre, and the other when it was rotated 22° around an axis perpendicular to the axis of the fibre.

In both cases, the interference figures were photographed with the same lamellar fragment as was used in the case of Fig. 12, Plate II. The distance between the photographic plate and the specimen was 3.5 cm. If our consideration be correct, the figure in the former case should remain unaltered; while in the latter case the symmetry of the figure should be violated. As was expected, the interference figure, essentially the same as Fig. 12, Plate II, was obtained in the former case, but in the latter the interference figure was quite different from the former one. Fig. 18, Plate III is the photograph taken when the axis of the fibre was tilted from its vertical position toward the incident ray.

The full lines in Fig. 3 represent the radiating bands calculated from the consideration stated above, and the shaded part in this figure is the copy of the diffraction pattern in Fig. 18, Plate III (Fig. 3 in the position rotated about 80° in the plane of the paper). In these figures

Fig. 3.

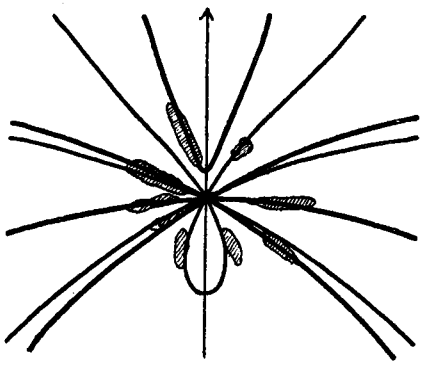

the direction represented by the arrow indicates the line of intersection of the surface of the photographic plate with the plane containing the incident X-ray-beam and the direction of the axis of the fibre in the specimen. The thick full lines in Fig. 3 are the calculated curves corresponding to $\beta=18^\circ\ 20'$, $\beta=63^\circ\ 21'$ and $\beta=90^\circ$. These lines are to be caused by the reflection from the most prominent atomic planes of the indices $(1\ 1\ 1)$ and $(1\ 1\ \bar{1})$, and they correspond to the strongest bands marked by I_1 and I_2 in the case of the normal incidence of the X-rays to the lamellar surface of the specimen. The thin full lines are the calculated curves corresponding to $\beta=38^\circ\ 2'$ and $\beta=66^\circ\ 48'$, and they correspond to the bands marked by II in the case of normal incidence, whose intensities are next to those marked by I_1 and I_2. As may be seen from Fig. 3, the agreement between the calculated curves and the observed ones is satisfactory.

Accordingly, our foregoing consideration is again confirmed, and we may conclude that a crystal-axis of the indices $[2\ 1\ 1]$ is arranged in a direction parallel to the axis of the fibre.

(iii) On the Formation of Laue's Spots:

It was already stated that the acicular specimen belonging to Specimen A_3 of *Bi* is supposed to be an aggregation of crystals of considerable size. The further arguments we now attempt to make, aim to determine the orientation of each crystal in this specimen, with respect to the direction of the acicular axis. This determination was easily carried out from the positions of Laue's spots as in Fig. 13, Plate II, by making use of the Yoshida globe and spherical scale; and it was found in the case of Fig. 13, Plate II, that only when the direction of the incident beam inclines 48°, 27° and 18° respectively to the normals to the atomic planes $0\ 1\ 1$, $0\ 0\ 1$, and $1\ 0\ \bar{1}$, was the distribution of Laue's spots found to agree well with that of Fig. 13, Plate II. This relation is shown in Fig. 4. Considering this to be correct, and if we take into account the atomic planes of a small glancing angle only (less than 20°), it can be expected that each one of the atomic planes $1\ 1\ 1$, $1\ 0\ 1$, and $1\ \bar{1}\ 1$, will give rise to a very intense spot. As was expected, three spots represented respectively by a, b, and c in Fig. 13, Plate II, came to appear just at the positions where the reflected beams from the atomic planes $1\ 1\ 1$, $1\ 0\ 1$, and $1\ \bar{1}\ 1$ were to be registered. Thus, we may conclude that the direction of the incident beam is parallel to the direction $\overrightarrow{PQO}$ in Fig. 4.

Fig. 4.

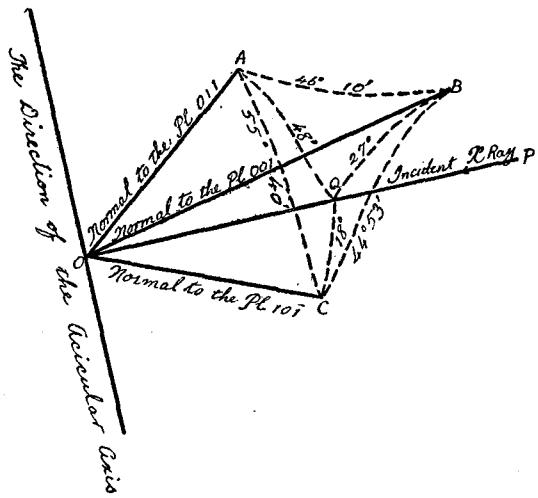

Here, it should be noticed that this direction $\vec{PQO}$ is normal to the crystal-axis of the indices [2 1 1], and that Fig. 13, Plate II is a diffraction figure produced by the normal incidence of the X-ray-beam to the acicular axis of the specimen. Accordingly, if the azimuth of the acicular direction measured from a certain standard line (e. g., the line *Oa*) in Fig. 13, be equal to that measured on the globe by taking the direction $\vec{PQO}$ in Fig. 4 as the pole, then it can be concluded that the crystal axis of the indices [2 1 1] is orientated parallel to the direction of the acicular axis. As was observed from Fig. 13, Plate II, the angle between the direction of the acicular axis which is represented by an arrow and that of the line *Oa* amounts to 18°, while on the globe the azimuth of the axis [2 1 1] measured from the point corresponding to the atomic plane 1 1 1 on the globe is also 18°.

Accordingly, it may be concluded that in Specimen A_3 of *Bi* the crystal axis of the indices [2 1 1] are arranged parallel to the direction of the acicular axis, and that the diffraction figures Fig. 13, Plate II was produced by the normal incidence of the X-ray beam to the acicular axis.

Hitherto we have treated the diffraction pattern in Fig. 13, Plate II as an ordinary Laue's figure But, strictly speaking, it is not exactly so; and a slight elongation of each Laue's spots indicates the presence of a fibrous nature of weak degree.

To make clearer this point, it would be advisable to reconsider our argument which has previously been made in connection with Specimen A_2 of *Bi*. As was stated before, two different figures Figs. 12 and 14, Plate II were obtained with the samples belonging to this specimen. The former figure consists of several radiating bands; while in the latter not only several radiating bands, but a number of concentric rings are detectable. This shows us that the micro-crystals in the sample, with which the latter figure Fig. 14, Plate II was produced, is rather irregularly arranged compared with the other sample which is responsible for the former figure, Fig. 12, Plate II.

Furthermore, it can be noticed that the radiating bands themselves are of different nature in both figures; in Fig. 14, a number of long radiating bands come to appear symmetrically with respect to the direction of the fibrous axis. On the other hand, it is observed that the radiating bands are comparatively short and the symmetry of their angular distribution is violated to some extent in the case of Fig. 12, Plate II. This shows us that, in the case of Fig. 12, II, the rotation of the micro-crystals of bismuth around the axis of the fibre is less than in the case Fig. 14, Plate II.

This tendency is more remarkable in the acicular Specimen A_3 of *Bi*, which gave rise to Fig. 13, Plate II. The rotation of the micro-crystals around the axis of the fibre became so small, in this case, that the specimen can be looked for almost as a single crystal. The angle of rotation of the micro-crystals around the axis [2 1 1] was obtained by means of the Yoshida globe and spherical scale; and it was estimated to be within 10° in this case.

Summary.

From our foregoing argument in connection with electrolysed bismuth and antimony, we arrive at the following conclusions:—

(1) The smaller current density and the lower concentration of the electrolyte seem to be the more favourable conditions for the formation of a regular arrangement of bismuth crystals.

When the current density and the concentration of the electrolyte are comparatively large, the micro-crystals of bismuth have not a remarkable tendency to deposit themselves in a fibrous form. But, this tendency becomes more remarkable with a smaller current density and with a smaller concentration of the electrolyte; and a perfect fibrous arrangement

is at last obtained, when both of them are reasonably small. In the extreme case, when the current density and the concentration of the electrolyte are very small, the micro-crystals tend to form a crystal of considerable size, having not only a certain crystal-axis but all the crystal-axes coinciding with each other.

(2) The non-metallic cloddy deposits found on the cathode by the electrolysis of bismuth or antimony, are at least mainly composed of substances having the same crystal-lattices as those of bismuth or of antimony.

(3) The micro-crystals of bismuth in the fibrous specimens are so arranged that their crystal-axis of the indices [2 1 1] is parallel to the fibrous axis. In the case of the bismuth-single-crystals of acicular form, the same crystal axis [2 1 1] is also parallel to the direction of the acicular axis. Thus it may be said that the axis [2 1 1] of the rhombahedral crystal of bismuth has a distinct physical nature.

In conclusion, the writer wishes to express his best thanks to Prof. M. Chikashige for his kind suggestions and interest and to Professor U. Yoshida for his efficacious guidance during the progress of the experiment. His thanks are also due to Mr. J. Tsutsumi, by whose kind advice some of the specimens were prepared.

Plate I

Fig. 5, Bi. Specimen A_2

×75

Fig. 6, Bi. Specimen A_1

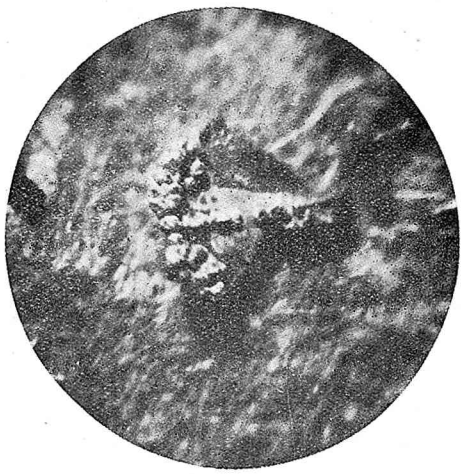

×75

Fig. 7, Sb. Specimen B_2

×140

Fig. 8, Sb. Specimen A_1

×75

Fig. 9, Bi. Specimen B_1

×40

Fig. 10, Bi. Specimen A_3

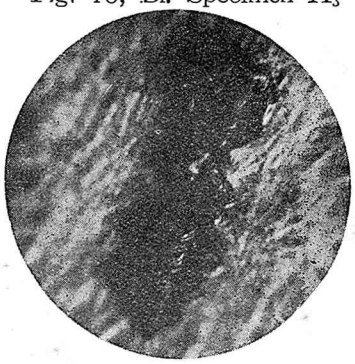

×75

Plate II

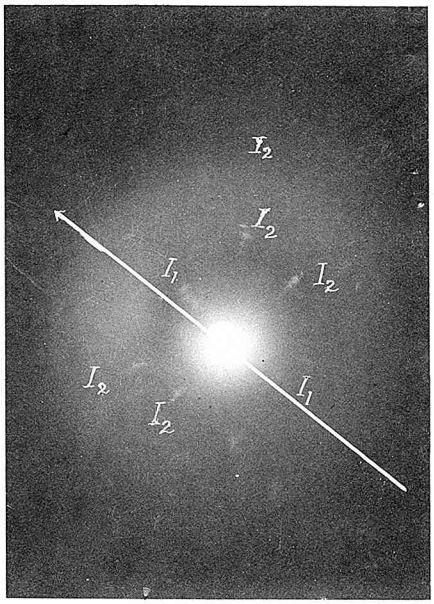

Fig. 11, Bi. Specimen A_1

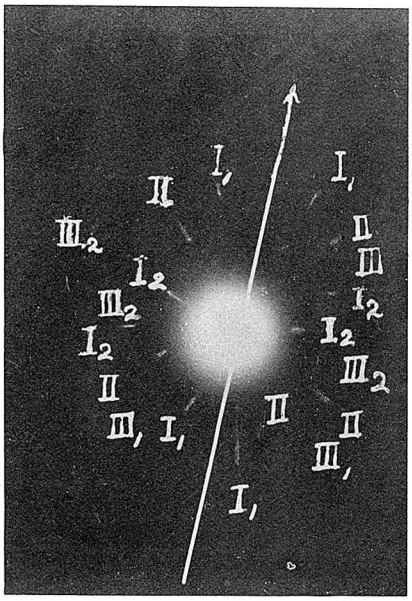

Fig. 12, Bi. Specimen A_2

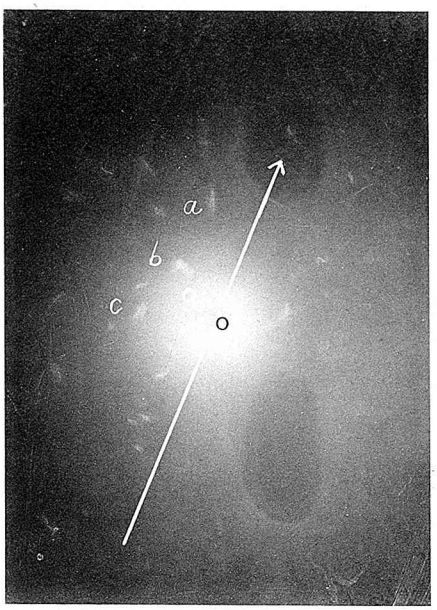

Fig. 13, Bi. Specimen A_3

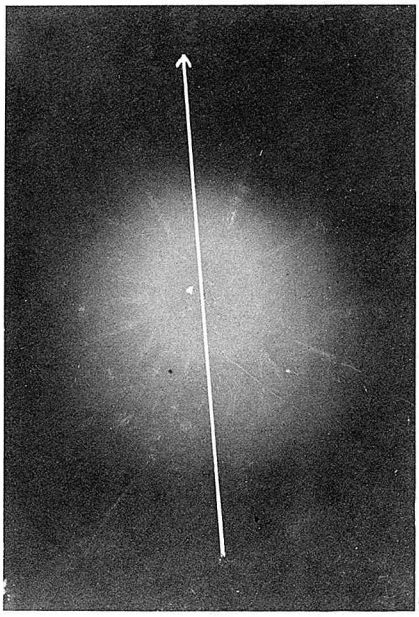

Fig. 14, Bi. Specimen A_2

Plate III

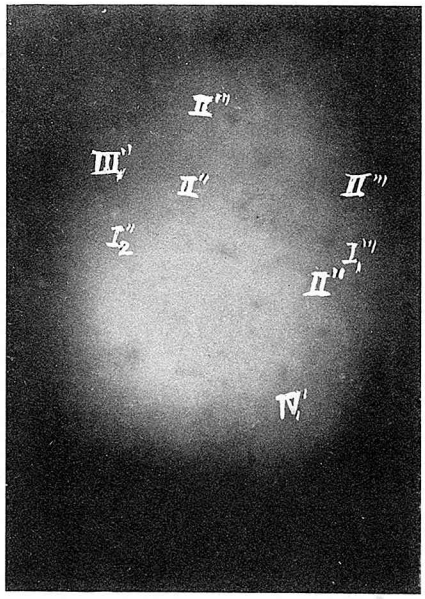

Fig. 15, Sb. Specimem A_2

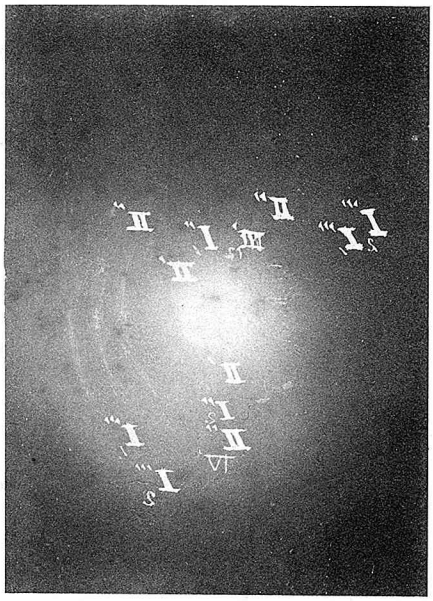

Fig. 16, Sb. Specimen B_1

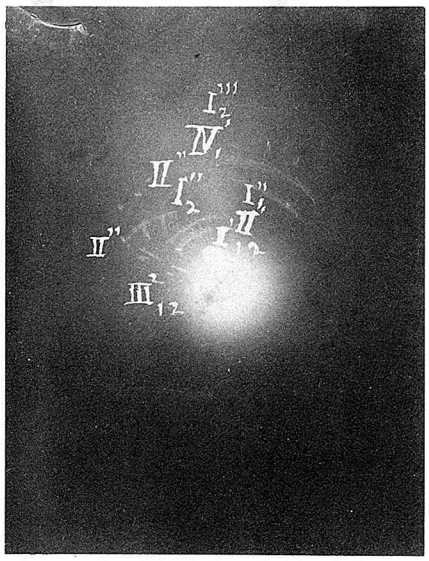

Fig. 17, Bi. Specimen B4

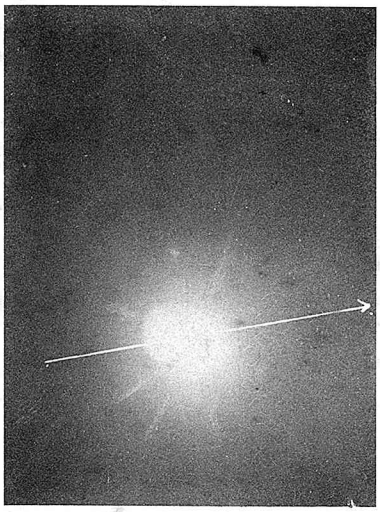

Fig. 18, Bi. Specimen A_2